A 0.6–3.8 GHz GaN Power Amplifier Designed Through a Simple Strategy

A 0.6–3.8 GHz GaN Power Amplifier Designed Through a Simple Strategy

Jorge Julian Moreno Rubio, Vittorio Camarchia, *Senior Member, IEEE*, Roberto Quaglia, *Member, IEEE*, Edison Ferney Angarita Malaver, and Marco Pirola, *Member, IEEE*

***Abstract*—This letter presents the design strategy for an ultra-wideband, high-efficiency hybrid power amplifier based on a commercial GaN-HEMT. The measurement results demonstrate a state-of-the-art fractional bandwidth of 145.5%, with saturated output power higher than 10 W from 0.6 to 3.8 GHz and power added efficiency exceeding 46% in the whole band, thus covering most of the mobile frequencies and making this device suitable for small-base station applications. The simple design approach exploits a N-section transformer, and allows for *a priori* estimation of the bandwidth: in the proposed case, a good agreement between estimated and measured bandwidth is obtained.**

***Index Terms*—Broadband matching networks, GaN-based FETs, wideband microwave amplifiers.**

I. Introduction

PRESENT mobile communication systems work from 800 MHz to roughly 3.5 GHz, with a trend to reach up to 5 GHz for broadband applications [1]. This means, if a single multi-application, broadband RF front-end is desired, that a fractional bandwidth exceeding 100% is needed. The power amplifier (PA), under this aspect, often represents the bottleneck of the RF front-end, due to the need to provide both high efficiency and large bandwidth.

For PAs with output power around 10 W, examples of ultra-octave designs are available, see Table I. In [2], a wideband PA with 112% of fractional bandwidth has been designed via real frequency technique. A 87% fractional bandwidth is reported in [3], where a specific filter topology has been adopted, and in [4] 11% more than one octave has been reached. The work of [5] achieves a PAE higher than 64% on the 2–3.5 GHz band, thanks to proper harmonic tuning, while [6] focuses on maintaining good gain flatness on the 2–4 GHz band.

This letter presents a wideband high efficiency PA adopting a 10 W GaN HEMT packaged active device. Being based on very simple device modelling and matching network synthesis, the design flow relies on plain calculations and passive network simulations only. Despite these simplifications, the measured results in terms of bandwidth and output power are well predicted in the design phase. The amplifier CW characterization shows Power Added Efficiency (PAE) from 46% to 75% and more than 10 W of saturated output power in a 145.5% fractional bandwidth from 0.6 to 3.8 GHz. Table I shows that this work favourably compares with the previously cited PAs, presenting a larger bandwidth, with full usage of the 10 W capability of the device.

TABLE I
State of the Art of Medium Power RF Wideband Power Amplifiers

Ref.	Central Freq. (GHz)	BW (%)	Gain (dB)	P_{OUT} (W)	PAE (%)
[2]	1.95	112	10-14	9.1-20.4	52-85
[3]	1.8	87	10-13	10-11	59-79
[4]	3.1	78	9-11	10-15	50-63
[5]	2.75	78	N.A.	11.2-15.8	N.A.
[6]	3.0	67	11.1-12.6	10	37-53
This work	2.2	145.5	9-14	10-15.5	46-75

II. Design

A. Design Strategy

The major issue in the realization of high efficiency ultra-octave microwave PAs is the variation of the optimum load vs. frequency, due to the reactive effects of the device. For this reason, this work is focused on the output matching network (OMN) design, that for the used device relies on a simple strategy. The input matching is based on a trade-off between minimum reflection and gain equalization, but it can be modified, according to the system specifications, with minor impact on the power and efficiency performance.

The adopted device is the CGH40010 10 W packaged transistor from Cree Inc, with drain bias voltage of 28 V. Observing the load pull data provided by the datasheet, the intrinsic optimum load $R_{\rm int}$ is around 30 Ω, and the reactive effects can be modelled by shunt capacitance $C_{\rm OUT} = 1.27$ pF and series inductance $L_{\rm OUT} = 0.63$ nH [4], [7].

Fig. 1 shows the load $Z_L(f)$ at the drain pin needed to present $R_{\rm int}$ at the intrinsic drain plane in the 0.5 to 4.5 GHz frequency range (covering most of the mobile applications).

From Fig. 1, it is worth to notice that a significant part of the load trajectory $Z_L(f)$ is located on the second quadrant of the reflection coefficient plane $\Gamma_L = (Z_L(f) - Z_0)/(Z_L(f) + Z_0)$. This condition is verified for the majority of devices,

Manuscript received November 11, 2015; revised January 26, 2016; accepted February 16, 2016. Date of publication May 12, 2016; date of current version June 3, 2016.

J. J. Moreno Rubio and E. F. Angarita Malaver are with the Department of Electronics, Universidad Pedagógica y Tecnológica de Colombia, 150003 Sogamoso, Colombia (e-mail: jorgejulian.moreno@uptc.edu.co).

V. Camarchia and M. Pirola are with the Department of Electronics, Politecnico di Torino, 10129 Torino, Italy (e-mail: vittorio.camarchia@polito.it).

R. Quaglia is with the Centre for High Frequency Engineering, Cardiff University, Cardiff, CF24 3AA Wales, U.K. (e-mail: quagliar@cardiff.ac.uk).

Color versions of one or more of the figures in this letter are available online at http://ieeexplore.ieee.org.

Digital Object Identifier 10.1109/LMWC.2016.2549263

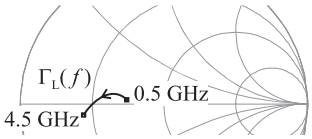

Fig. 1. External load Z_L to get the optimal intrinsic $R_{\rm int}$ for the CGH40010.

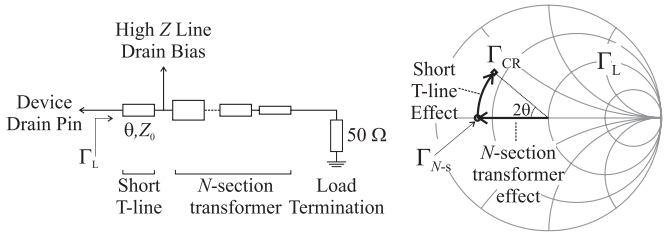

Fig. 2. Proposed OMN and implemented matching trajectories.

since output capacitance is usually dominant. At the frequency $f_0 = 2.5$ GHz, the value of $\Gamma_L(f_0)$ is located on the second quadrant of the Smith Chart, and it becomes the here-called Constant Relative optimal load $\Gamma_{\rm CR} = \Gamma_L(f_0)$. Fig. 2 shows the schematic of the OMN and the impedance transformation strategy. The N-section transformer converts the 50 Ω load into $\Gamma_{N-{\rm s}} = -|\Gamma_{\rm CR}|$, located on the negative real semi-axis. Since the transformer bandwidth can be set arbitrarily large by increasing the number of sections, the provided $\Gamma_{N-{\rm s}}$ can be considered constant. Rotating at constant reflection coefficient modulus, $\Gamma_{\rm CR}$ is synthesized at $f_0 = 2.5$ GHz inserting a transmission line with impedance Z_0 and electrical length $\theta = (\pi - \arg(\Gamma_{\rm CR}))/2$ at 2.5 GHz. The relatively short length of this line limits the frequency dispersion of the synthesized load, keeping it close to its optimum trajectory. The frequency behavior of the synthesized load $Z_{L,S}(f)$ due to transmission line phase effects is

$$Z_{L,S}(f) = Z_0 \frac{1 - |\Gamma_{\rm CR}| e^{-j2\theta\frac{f}{f_0}}}{1 + |\Gamma_{\rm CR}| e^{-j2\theta\frac{f}{f_0}}}. \tag{1}$$

Finally, the expression of device intrinsic termination $Z_{{\rm int},S}(f)$ as a function of frequency is given by

$$Z_{{\rm int},S}(f) = \frac{\frac{1}{j2\pi f C_{\rm OUT}} \left(j2\pi f L_{\rm OUT} + Z_{L,S}(f)\right)}{\frac{1}{j2\pi f C_{\rm OUT}} + j2\pi f L_{\rm OUT} + Z_{L,S}(f)}. \tag{2}$$

B. Bandwidth Estimation

The dynamic load curve slope depends on the magnitude of the synthesized intrinsic fundamental load, which is function of frequency and can be calculated from (2). The effect of the harmonic terminations has been neglected: $C_{\rm OUT}$ reduces the impact of out-of-band harmonic loads, while in-band loads are similar to the fundamental ones, thus not high enough to significantly affect the drain voltage waveforms.

In this framework, assuming that saturation has been reached and a bias point near to class B has been adopted,

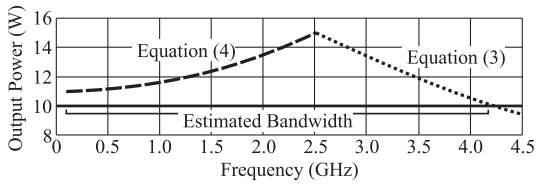

Fig. 3. Output power vs. frequency calculated with (3) (dashed line) and (4) (dotted line). The bandwidht estimation is highlighted.

if $|Z_{{\rm int},S}(f)| > R_{\rm int}$ (early voltage saturation), the estimated amplifier output power can be calculated as

$$P_{\rm OUT}(f) = \frac{1}{8} \left| \frac{R_{\rm int} I_{\rm MAX}}{Z_{{\rm int},S}(f)} \right|^2 \Re\left(Z_{{\rm int},S}(f)\right) \tag{3}$$

with $I_{\rm MAX} = 2$ A. Conversely, if $|Z_{{\rm int},S}(f)| < R_{\rm int}$ (early current saturation), the amplitude of the fundamental drain current is $I_{\rm MAX}/2$, and the output power is estimated as

$$P_{\rm OUT}(f) = \frac{|I_{\rm MAX}|^2}{8} \Re\left(Z_{{\rm int},S}(f)\right). \tag{4}$$

Expressions (3) and (4) allow to relate the amplifier bandwidth with the minimum output power target. Considering the nominal 10 W of the device and the estimated $Z_{{\rm int},S}(f)$, it can be seen that, for frequencies lower than 2.5 GHz, the magnitude of $Z_{{\rm int},S}(f)$ is lower than $R_{\rm int} = 30$ Ω, whereas for frequencies higher than 2.5 GHz the magnitude is higher. In this way, (4) is applied for the former and (3) for the latter case, respectively, and the results are plotted in Fig. 3. The bandwidth is defined as the range of frequencies where the output power is higher than 10 W (100% of power utilization factor for the selected device). As it can be noticed, the estimated bandwidth extends from very low frequencies up to 4.2 GHz. In Fig. 3, the extension of the bandwidth down to dc is an artifact due to considering infinite the bandwidth of the multi-section transformer. However, for real applications, a sufficiently low frequency can be achieved with reasonable number of sections.

III. Realization and Experimental Characterization

A Chebyshev transformer with two quarterwave sections was adopted. If compared to a three section realization, it gives comparable performance with a smaller circuit size.

Fig. 4 reports $\Gamma_{{\rm int},S}(f)$, defined as

$$\Gamma_{{\rm int},S}(f) = \frac{Z_{{\rm int},S}(f) - R_{\rm int}}{Z_{{\rm int},S}(f) + R_{\rm int}} \tag{5}$$

in the two cases where $Z_{{\rm int},S}$ is calculated with (2), or synthesized by the simulated matching network (including the bias elements), respectively.

The distributed input matching network minimizes the reflections in large signal conditions [7]. Broadband stability is analysed through small signal parameters sweeping the bias current up to class A. In-band stability is guaranteed by a parallel R/C in series to the gate, while gate bias resistors perform low frequency stabilization. The full PA scheme is shown

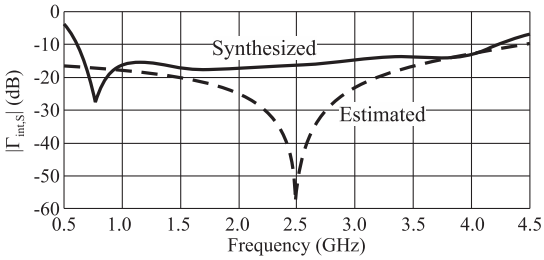

Fig. 4. Reflection coefficient $\Gamma_{\mathrm{int},S}$ vs. frequency, obtained at the intrinsic reference plane using the proposed OMN. Estimated (dashed line) and synthesized (solid line).

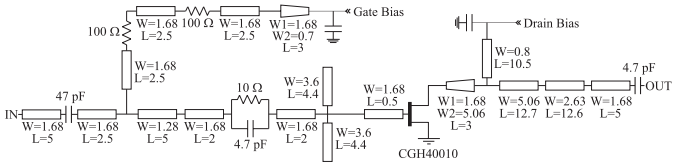

Fig. 5. Schematic of the designed PA. Dimensions are in mm.

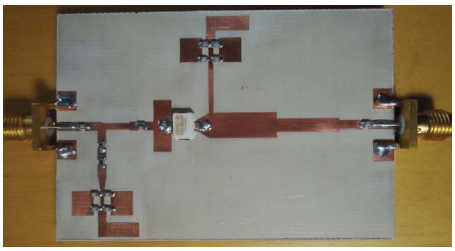

Fig. 6. Picture of the realized wideband PA. Size: 69×40 mm^2.

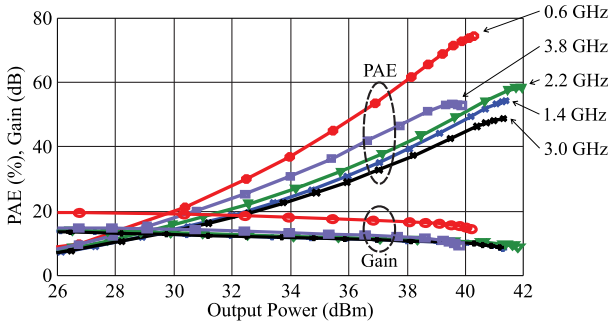

Fig. 7. Measured PAE vs. output power for some in-band frequencies.

in Fig. 5. The amplifier is fabricated on a Taconic substrate with copper metallization (RF35 with $\epsilon_r = 3.5$, substrate height $H = 0.76$ mm, and metal thickness $t = 0.035$ mm), mounted on a brass carrier, see Fig. 6. At the OMN, the short transmission line has been changed for a short taper in order to generate soldering space, but with negligible effects on the performance. Bias current is set at 150 mA for a flat gain vs. power response. Fig. 7 shows the measured Power Added Efficiency (PAE) vs. output power for some in-band frequencies, while the results in terms of saturated output power, saturated gain, efficiency and PAE vs. CW frequency are shown in Fig. 8. It can be noticed that the measured bandwidth for which the saturated

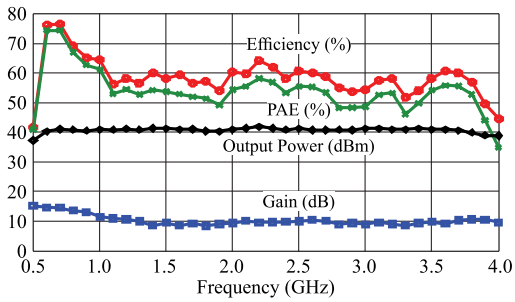

Fig. 8. Measured saturated gain, saturated output power, efficiency and PAE (at saturation) vs. frequency.

output power is higher than 10 W extends from 0.6 GHz to 3.8 GHz (fractional bandwidth of 145.5%). On the same band, the saturated gain is between 9 and 14 dB and the saturated PAE exceeds 46%. The band is well approximated by Fig. 3, except the expected cutting at low frequencies.

The linearity of the wideband PA has been tested using a 28 MHz channel OFDM signal, typical of LTE sytems, with 9.2 dB of peak-to-average power ratio (PAPR) at two frequencies, 2.6 GHz and 3.5 GHz. The resulting measured output power spectrum density without DPD shows, for an average power corresponding to ≈10 dB OBO, an adjacent channel leakage ratio (ACLR) around 33 dBc, whereas an ACLR of 46 dBc compliant with the LTE requirement of 45 dB is obtained through odd polynomial digital pre-distortion, The average efficiency is 26% at 2.6 GHz and 20% at 3.5 GHz.

IV. Conclusion

A state-of-the-art wideband high efficiency PA has been designed and characterized using a simple methodology that exploits N-section transformers. A fractional bandwidth of 145.5% together with 10 W of output power and saturated gain between 9 and 14 dB have been obtained.

References

[1] S. Chen, Y. Wang, F. Qin, Z. Shen, and S. Sun, "LTE-HI: A new solution to future wireless mobile broadband challenges and requirements," *IEEE Trans. Wireless Commun.*, vol. 21, no. 3, pp. 70–78, Jun. 2014.

[2] Z. Dai, S. He, F. You, J. Peng, P. Chen, and L. Dong, "A new distributed parameter broadband matching method for power amplifier via real frequency technique," *IEEE Trans. Microw. Theory Techn.*, vol. 63, no. 2, pp. 449–458, Feb. 2015.

[3] K. Chen and D. Peroulis, "Design of broadband highly efficient harmonic-tuned power amplifier using in-band continuous class- F^{-1}/F mode transferring," *IEEE Trans. Microw. Theory Techn.*, vol. 60, no. 12, pp. 4107–4116, Dec. 2012.

[4] P. Saad, C. Fager, H. Cao, H. Zirath, and K. Andersson, "Design of a highly efficient 2–4-GHz octave bandwidth GaN-HEMT power amplifier," *IEEE Trans. Microw. Theory Techn.*, vol. 58, no. 7, pp. 1677–1685, Jul. 2010.

[5] J. Xia, X.-W. Zhu, and L. Zhang, "A linearized 2–3.5 GHz highly efficient harmonic-tuned power amplifier exploiting stepped-impedance filtering matching network," *IEEE Microw. Wireless Compon. Lett.*, vol. 24, no. 9, pp. 602–604, Sep. 2014.

[6] X. Ding, S. He, F. You, S. Xie, and Z. Hu, "2–4 GHz wideband power amplifier with ultra-flat gain and high PAE," *Electron. Lett.*, vol. 49, no. 5, pp. 326–327, Feb. 2013.

[7] J. M. Rubio, J. Fang, V. Camarchia, R. Quaglia, M. Pirola, and G. Ghione, "3–3.6 GHz wideband GaN Doherty power amplifier exploiting output compensation stages," *IEEE Trans. Microw. Theory Techn.*, vol. 60, no. 8, pp. 2543–2548, Aug. 2012.